

**Rocking feedback-controlled ratchets**

M. Feito\*

*Departamento de Física Atómica, Molecular y Nuclear, Universidad Complutense de Madrid,  
Avenida Complutense s/n, 28040 Madrid, Spain*

J. P. Baltanás†

*Departamento de Física Aplicada II, Universidad de Sevilla, Av. Reina Mercedes 2, 41012 Sevilla, Spain*

F. J. Cao‡

*Departamento de Física Atómica, Molecular y Nuclear, Universidad Complutense de Madrid,  
Avenida Complutense s/n, 28040 Madrid, Spain  
and LERMA, Observatoire de Paris, Laboratoire Associé au CNRS UMR 811 2,  
61 Avenue de l'Observatoire, 75014 Paris, France*

(Received 23 February 2009; revised manuscript received 22 May 2009; published 21 September 2009)

We investigate the different regimes that emerge when a periodic driving force, the rocking force, acts on a collective feedback flashing ratchet. The interplay of the rocking and the feedback control gives a rich dynamics with different regimes presenting several unexpected features. In particular, we show that for both the one-particle ratchet and the collective version of the ratchet an appropriate rocking increases the flux. This mechanism gives the maximum flux that has been achieved in a ratchet device without an *a priori* bias.

DOI: [10.1103/PhysRevE.80.031128](https://doi.org/10.1103/PhysRevE.80.031128)

PACS number(s): 05.40.-a, 05.60.Cd

**I. INTRODUCTION**

Ratchets can be viewed as controllers that act on stochastic systems with the aim of inducing directed motion by breaking of thermal equilibrium and certain time-space symmetries [1]. As usual in control theory [2], these systems are divided into *open-loop* ratchets [1], when the actuation does not use any knowledge of the state of the system; and *closed-loop* ratchets [3,4], when information on the state of the system is used to decide how to operate on the system. These closed-loop ratchets—also called feedback or information ratchets—have recently attracted attention as Maxwell's demon devices that are capable of maximizing the performance of ratchets [5]. They may also be relevant to get insight into the motion of linear, two headed, processive molecular motors [6]. In addition, experimental realizations of feedback ratchets have been recently proposed [3,7] and implemented [8] due to their potential relevance as nanotechnological devices.

A relevant class of ratchets are *flashing* ratchets, which operate switching on and off a spatially periodic potential. Flashing ratchets have been studied in both open-loop (e.g., [1,9]) and closed-loop (e.g., [3,4,10]) schemes. A generalization of these ratchets are pulsed ratchets [1], in which the amplitude of the ratchet potential is modulated in time, but not necessarily flashed on and off. On the other hand, *rocking* ratchets operate thanks to a periodic driving force, and thus they perform an open-loop control. Rocking ratchets reveals a rich dynamics, which includes current reversals, distinct stable trajectories, and quantization of the determin-

istic current [11–13]. The combination of open-loop pulsed ratchets and rocking ratchets has been studied in Ref. [14], giving the possibility of a reverse of the sign of the flux with respect to the simple rocked ratchet.

In the present paper we study the effects of adding a periodic driving force that rocks a feedback-controlled flashing ratchet. We analyze the intriguing dynamics that emerge due to the interplay between the feedback control and the rocking. In particular, we show that the rocking of a feedback ratchet allows the system to improve the flux performance. The optimization of the flux performance of ratchets is potentially relevant for their nanotechnological applications, and the enhancement of the flux performance in flashing ratchets due to feedback has been recently verified experimentally [8]. We show here how this flux performance can be further improved thanks to the effects produced by an additional rocking force. In the next section we describe the rocked feedback-controlled ratchet, and after, in Sec. III, we study the one-particle ratchet. The collective version of the ratchet compounded of more than one particle is analyzed in Sec. IV in the regimes of few and many particles. We finally summarize and comment our main results in Sec. V.

**II. ROCKED FEEDBACK-CONTROLLED RATCHET**

Let us consider  $N$  Brownian particles at temperature  $T$  in a periodic potential  $V(x)$ , the ratchet potential. The state of the system is described by the positions  $x_i(t)$  of the particles ( $i=1, \dots, N$ ) satisfying the overdamped Langevin equations with a fluctuating (rocking) force of amplitude  $A$  and frequency  $\Omega$ ,

$$\gamma \dot{x}_i(t) = \alpha(x_1(t), \dots, x_N(t), t) F(x_i(t)) + A \cos(\Omega t) + \xi_i(t). \quad (1)$$

Here,  $F(x) = -V'(x)$ ,  $\gamma$  is the friction coefficient (related to the diffusion coefficient  $D$  through Einstein's relation  $D$

\*feito@fis.ucm.es

†baltanas@us.es

‡franco@fis.ucm.es

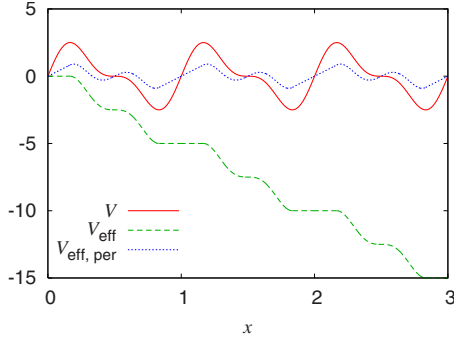


FIG. 1. (Color online) Ratchet potential  $V$  (solid red line) [Eq. (5) with  $V_0=5$ ], one-particle effective potential  $V_{\text{eff}}$  (dashed green line), and one-particle periodic effective potential  $V_{\text{eff}}^{\text{per}}$  (dotted blue line). Units:  $k_B T=1$ ,  $L=1$ .

$=k_B T/\gamma$ ), and  $\xi_i(t)$  are Gaussian white noises of zero mean and variance  $\langle \xi_i(t)\xi_j(t') \rangle = 2\gamma k_B T \delta_{ij} \delta(t-t')$ . Note that the control parameter  $\alpha$  depends explicitly on the state of the system. Therefore, this ratchet is feedback controlled, what implies an effective coupling between the particles.

In order to quantify the induced directed motion a relevant quantity is the stationary center-of-mass velocity or flux defined as

$$\langle \dot{x} \rangle := \lim_{t \rightarrow \infty} \frac{1}{N} \sum_{i=1}^N \frac{\langle x_i(t) - x_i(0) \rangle}{t} = \lim_{t \rightarrow \infty} \frac{1}{N} \sum_{i=1}^N \frac{\langle x_i(t) \rangle}{t}. \quad (2)$$

Due to the long-time limit and the average over realizations this asymptotic center-of-mass velocity does not depend neither on the phase of the fluctuating force nor on the initial particle positions [1]. We shall consider the relevant control policy that maximizes the instant center-of-mass velocity introduced in [4]. In this feedback protocol, the controller computes the force per particle due to the ratchet potential if it were on,

$$f(x_1(t), \dots, x_N(t)) = \frac{1}{N} \sum_{i=1}^N F(x_i(t)), \quad (3)$$

and switches the potential on ( $\alpha=1$ ) if  $f(t)$  is positive or switches the potential off ( $\alpha=0$ ) otherwise. Therefore, the feedback control protocol considered is

$$\alpha(x_1(t), \dots, x_N(t)) = \Theta(f(x_1(t), \dots, x_N(t))), \quad (4)$$

with  $\Theta$  the Heaviside function [ $\Theta(x)=1$  if  $x>0$ , else  $\Theta(x)=0$ ].

The graphs that illustrate the results of this paper have been obtained considering the periodic asymmetric potential

$$V(x) = \frac{2V_0}{3\sqrt{3}} \left[ \sin\left(\frac{2\pi x}{L}\right) + \frac{1}{2} \sin\left(\frac{4\pi x}{L}\right) \right], \quad (5)$$

which has potential height  $V_0$  and period  $L$ ; see Fig. 1. We can introduce an asymmetry parameter  $a$  for the potential such that  $aL$  is defined as the distance between a minimum of the potential and the first maximum at the right-hand side. The potential in Eq. (5) has an asymmetry parameter of  $a$

$=1/3$ . We have also performed computations with other potentials and found analogous results.

In order to numerically compute flux (2) we have performed numerical simulations of the Langevin Eq. (1) [with the control parameter  $\alpha$  given by Eq. (4)] by using the Euler-Maruyama algorithm [15]. We have verified that our numerical results were not affected by systematic errors due to time discretization, initial transients or finite number of realizations. The characteristic time that takes the system to diffuse the distance  $aL$  of the uphill part of the ratchet potential is  $a^2 L^2 / (2D)$ , while the characteristic time that takes to “slide down” the downhill part of the potential is  $\gamma(1-a)^2 L^2 / V_0$ . Therefore, the discretization time has been chosen much smaller than these times, and also much smaller than the period of the rocking,  $2\pi/\Omega$ , to avoid aliasing. In addition, the Langevin equations have been numerically solved up to times much greater than these characteristic times, and large enough to ensure a value of the computed flux close to its asymptotic value independently of the specific realization of the stochastic process, the initial conditions, or the initial transients. We have performed the number of realizations required to have small statistical errors in the averages computed.

### III. ONE-PARTICLE RATCHET

For the one-particle ratchet ( $N=1$ ), the maximization of the instant velocity control policy [Eq. (4)] only depends of the position  $x(t)$  of the particle. Hence, we can define an effective force  $F_{\text{eff}}(x) = \alpha(x)F(x)$  that allows us to rewrite Langevin Eq. (1) as

$$\gamma \dot{x}(t) = F_{\text{eff}}(x(t)) + A \cos(\Omega t) + \xi(t). \quad (6)$$

The effective force  $F_{\text{eff}}$  derives from an effective potential  $V_{\text{eff}}(x)$  that is no longer periodic, but tilted downhill. This  $V_{\text{eff}}$  can be recast as a periodic potential  $V_{\text{eff}}^{\text{per}}(x)$  of height  $aV_0$  and asymmetry  $a$ , plus a linear term  $V_0 x/L$  accounting for the bias, where  $V_0$  is the height of the ratchet potential,  $a$  its asymmetry parameter, and  $L$  its period. Therefore, we can write  $V_{\text{eff}}(x) = V_{\text{eff}}^{\text{per}}(x) - V_0 x/L$ , as we illustrate in Fig. 1 for potential (5). In view of these considerations, the feedback rocking ratchet can be reinterpreted as an open-loop rocking ratchet with a biased asymmetric potential. Thus Eq. (6) stands for the celebrated superconducting quantum interference device (SQUID) ratchet [16],

$$\gamma \dot{x}(t) = - \frac{d}{dx} V_{\text{eff}}^{\text{per}}(x(t)) + V_0/L + A \cos(\Omega t) + \xi(t). \quad (7)$$

This equation of motion describes the dynamics of a tilted rocking ratchet, i.e., of a periodically driven single Brownian particle in a tilted washboard potential, and it has been extensively studied analytically and numerically [12,16,17] (even when inertial terms are also present [18]). For instance, for the adiabatic regime, i.e., the regime of slow driving [13], the flux can be approximated by

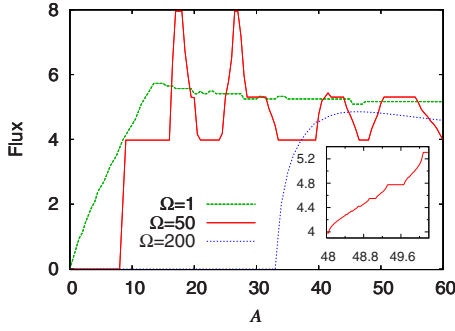


FIG. 2. (Color online) One-particle case. Flux for the deterministic (zero-temperature) rocked feedback ratchet as a function of the amplitude  $A$  of the rocking and frequencies  $\Omega=1, 50, 200$  for the ratchet potential of Fig. 1. Inset: zoom of the flux for  $\Omega=50$  and  $A$  belonging to the interval  $[48.0, 50.2]$ . Units:  $V_0=5$ ,  $L=1$ , and  $\gamma=1$ .

$$\langle \dot{x} \rangle = \frac{1}{T} \int_0^T \langle \dot{x} \rangle_{G(t)} dt, \quad (8)$$

where  $T=2\pi/\Omega$  is the period of the driving force and  $\langle \dot{x} \rangle_{G(t)}$  is the asymptotic flux that would be obtained if the driving force were fixed at the instant  $t$  to its value  $G(t)=A \cos(\Omega t)$ . This flux can be obtained by solving a Fokker-Plank equation for the resulting constant external force [5]. Other analytical results have been reported for the high-frequency regime [19], or the deterministic (zero-temperature) regime [20]. Thanks to the equivalence found between the one-particle rocked feedback ratchet [Eqs. (1) and (4)] and the SQUID ratchet [Eq. (7)], all the effects found for the rocked feedback ratchet have their counterparts in the extensively studied SQUID ratchet. However, it is important to emphasize that the tilt appears in our results not as an *a priori* bias, but as part of an effective description of the effects of the feedback.

Here, we discuss the results for the different regimes obtained by performing numerical simulations of the Langevin equation. We shall first discuss the case of zero temperature and later the case of nonzero temperature.

In the deterministic case of zero temperature there is no diffusion and only the rocking force can help the particle to cross the flat regions of the effective potential  $V_{\text{eff}}$  (see Fig. 1). This makes the flux strictly zero for small amplitudes such that the particle cannot overcome the flat part of the effective tilted potential; see Fig. 2. For higher amplitudes the flux exhibits remarkable characteristic effects. Our simulations show that the deterministic flux is quantized and it presents a steplike structure, a well-known effect for open-loop rocking ratchets [16]. This structure is specially clear for the frequency  $\Omega=50$  in Fig. 2. The flux quantization is owing to the synchronization with the phase of the periodic driving (see [16] for details). Its steplike structure presents a self-similar structure with steps at rational values of the flux, which can be seen performing successive zoom-in views (see inset in Fig. 2). This structure is known as Devil's staircase [12,16].

Let us now discuss the case of nonzero temperature. A finite thermal noise leads to particle diffusion, which provides another mechanism to overcome the flat regions. This diffusion makes that the quantized steplike structure for the flux is smeared and finally wiped out. On the other hand, a surprising effect is found for this case, namely a flux increase when the feedback policy and the rocking forcing are both present. Unexpectedly, the resulting flux is greater than the sum of the flux values due to each separated effect, as we show in Fig. 3. In fact, the synchronization of the driving force with the feedback mechanism gives positive large fluxes even for the case of negative fluxes for the pure rocking, i.e., with the ratchet potential always on [compare, for instance, curves for  $A=40$  in panels (a) and (b) of Fig. 3, or curves for  $\Omega=100$  in panels of Fig. 4]. Therefore, adding an external fluctuating force to the maximization of the instant velocity feedback protocol allows us to improve the performance of the system in a nontrivial way which to our knowledge has not been previously reported. This fact is not only relevant from a theoretical point of view, but also for experimental ratchet devices designed to maximize the flux [3,8].

Further insight on the behavior observed in panel (a) of Figs. 3 and 4 can be obtained studying the fast driving regime. In this regime, it is useful to introduce a slow variable  $y(t)$  such that the position  $x(t)$  can be written as  $x(t)=y(t)+\psi(t)$ , where  $\psi(t)=r \sin(\Omega t)$  is the fast contribution due to

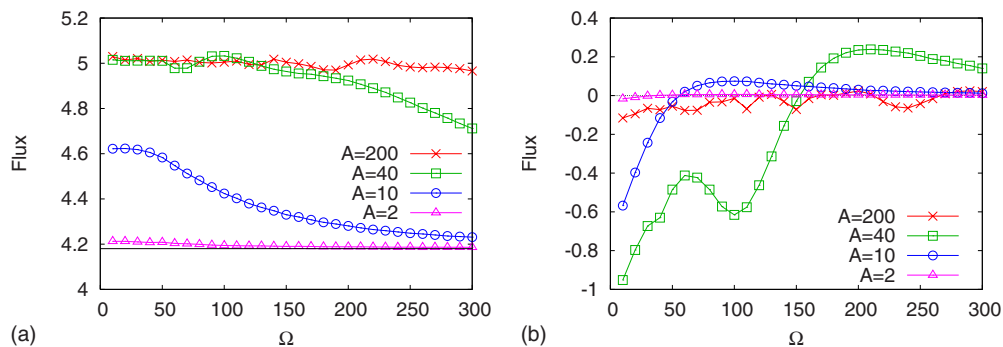


FIG. 3. (Color online) One-particle case. Panel (a): flux  $\langle \dot{x} \rangle$  versus frequency  $\Omega$  for the rocked feedback ratchet. The horizontal solid line stands for the pure feedback ratchet without rocking, i.e.,  $A=0$ . Panel (b): flux  $\langle \dot{x} \rangle$  versus frequency  $\Omega$  for the pure rocking ratchet without feedback flashing, i.e.,  $\alpha(t)=1$ . We have used the ratchet potential of Fig. 1. The one-sigma error bars are much smaller than the symbol size. Units:  $k_B T=1$ ,  $L=1$ , and  $\gamma=1$ .

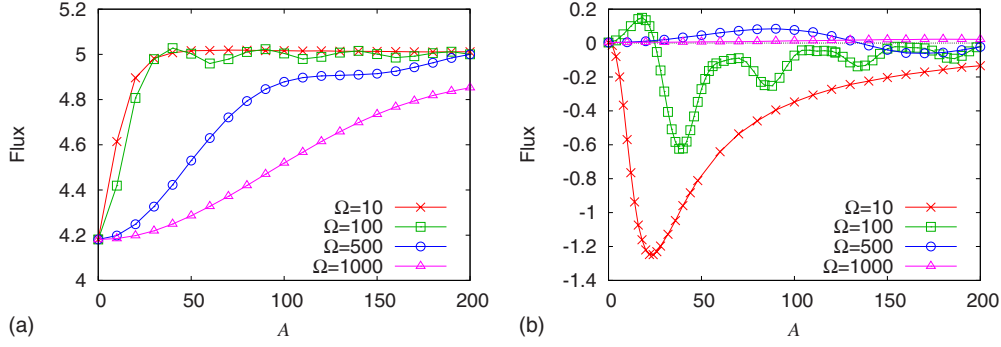


FIG. 4. (Color online) One-particle case. Panel (a): flux  $\langle \dot{x} \rangle$  versus amplitude  $A$  for the rocked feedback ratchet. The pure feedback ratchet—without rocking—corresponds to the point  $A=0$ . Panel (b): flux  $\langle \dot{x} \rangle$  versus amplitude  $A$  for the pure rocking ratchet without feedback flashing, i.e.,  $\alpha=1$ . We have used the ratchet potential of Fig. 1. The one-sigma error bars are much smaller than the symbol size. Units:  $k_B T=1$ ,  $L=1$ , and  $\gamma=1$ .

the fast driving, and  $r:=A/(\gamma\Omega)$ . When the driving is fast enough, a large number of oscillations in  $\psi(t)$  take place before a significant change in  $y(t)$  occurs; thus, we can proceed to the adiabatic elimination of the fast variable  $\psi(t)$  by averaging it over time. This procedure leads to an effective equation for the slow variable

$$\gamma \dot{y}(t) = \bar{F}_{\text{eff}}(y(t)) + \xi(t), \quad (9)$$

where  $\bar{F}_{\text{eff}}(y) = -\bar{V}'_{\text{eff}}(y)$ , with

$$\bar{V}_{\text{eff}}(y(t)) := \frac{1}{T} \int_0^T V_{\text{eff}}(y(t) + \psi(s)) ds. \quad (10)$$

This effective potential allows us to give a closed-form expression for the flux [1],

$$\langle \dot{x} \rangle = \frac{Lk_B T [1 - e^{(\bar{V}_{\text{eff}}(L) - \bar{V}_{\text{eff}}(0))/k_B T}]}{\gamma \int_0^L dx \int_x^{x+L} dy e^{(\bar{V}_{\text{eff}}(y) - \bar{V}_{\text{eff}}(x))/k_B T}}. \quad (11)$$

Note that the potential  $\bar{V}_{\text{eff}}(y(t))$  only depends on the characteristics of the driving force through the quotient  $r = A/(\gamma\Omega)$ , and hence the same is true for the flux obtained within this fast driving regime. This approach is known as

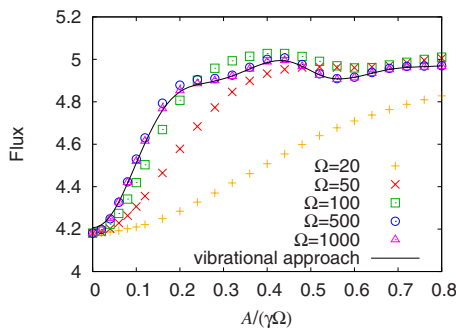


FIG. 5. (Color online) Flux  $\langle \dot{x} \rangle$  versus  $r = \frac{A}{\gamma\Omega}$  for the one-particle rocked feedback ratchet. For increasing frequencies the values of the flux tend to the curve of the vibrational approximation. We have used ratchet potential (5) with  $V_0=5$ . The one-sigma error bars are much smaller than the symbol size. Units:  $k_B T=1$ ,  $L=1$ , and  $\gamma=1$ .

the *vibrational mechanics* scheme [21]. It has been successfully applied to the characterization of the so-called vibrational resonance in bistable systems, both in the absence and presence of noise, as well as to the study of harmful effects (suppression of the firing activity) of strong, high-frequency fields on the response of excitable systems [22]. In the context of ratchets, it has been used in the study of the effects of high-frequency modulation on the output of Brownian particles moving in periodic one-dimensional substrates under the action of low-frequency input signals [23]. The results obtained with this vibrational mechanics procedure are valid when the rocking force has frequencies much larger than the rest of characteristic frequencies of the system [21]. The average in Eq. (10) makes the original potential barriers appear effectively lowered and flattened, eventually disappearing as the ratio  $r$  increases. In particular, in our system, the periodic part of the one-particle effective potential  $V_{\text{eff}}(x) = V_{\text{eff}}^{\text{per}}(x) - V_0 x/L$  becomes smoother and smoother as an effect of the averaging process as  $r$  grows, and for large  $r$  only the linear term survives in the effective potential, giving a flux value of  $V_0/(L\gamma)$ . Panel (a) of Figs. 3 and 4 and Fig. 5 show how this value is reached for large amplitudes. Indeed, this is the largest value of the flux that has been obtained in a ratchet device without an *a priori* bias; see Fig. 6.

The previous analysis also provides predictions on the dependency of the flux with the amplitude and frequency of the driving force. Within the vibrational regime, if the frequency is increased for a fixed amplitude, i.e.,  $r$  is decreased, then the flux will decrease until the value of the pure feedback ratchet [see panel (a) of Figs. 3 and 5]. Note that the values of the flux corresponding to low frequencies can be explained with the adiabatic description in Eq. (8). On the other hand, if the amplitude is increased for a fixed frequency, i.e.,  $r$  is increased, then the flux will increase from the value of the pure feedback ratchet up to the maximum value  $V_0/(L\gamma)$  [see panel (a) of Figs. 4 and 5].

The effective potential  $\bar{V}_{\text{eff}}$  has allowed us to describe the dynamics in the vibrational regime. We have compared the results obtained directly from Eqs. (10) and (11) with numerical simulations of Langevin Eq. (1), with a good agreement for the fast driving regime (Fig. 5). This stress again the significance of the vibrational approach that has been

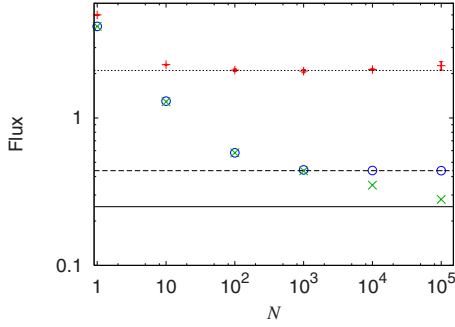


FIG. 6. (Color online) Maximum center-of-mass flux versus number of particles  $N$  for the optimal rocked feedback ratchet (red +), the optimal threshold protocol (blue  $\circ$ ), the instant maximization protocol—pure feedback—(green  $\times$ ), the optimal rocked flashing ratchet (dotted line), the optimal periodic protocol (dashed line), and the optimal rocking ratchet—pure rocking—(solid line). We have used ratchet potential (5) with  $V_0=5$ . Where not shown, the error bars are smaller than the symbol size. Units:  $k_B T=1$ ,  $L=1$ , and  $\gamma=1$ .

revealed as a useful approach for both qualitative and quantitative predictions. On the other hand, we have found that fluxes greater than  $V_0/(L\gamma)$  can be attained outside the vibrational regime in the quasideterministic regime, i.e., for large values of the potential height and the driving force amplitude. [For example, ratchet potential (5) with  $V_0=40$ , and a rocking force with  $A=160$  and  $\Omega=290$  gives  $\langle \dot{x} \rangle \approx 43$  in units  $k_B T=1$ ,  $L=1$ , and  $\gamma=1$ ]. This result is in accordance with the results found in Ref. [17] for a tilted rocking ratchet in the quasideterministic regime.

#### IV. COLLECTIVE RATCHET

The dynamics of the collective ratchet compounded of more than one particle differs significantly from that of the one-particle ratchet discussed before. For collective closed-loop ratchets the feedback effectively couples the particles with each other and no simplifying description in terms of an effective potential has been found.

The behavior of the deterministic (zero-temperature) collective ratchet is similar to that of the one-particle ratchet, including the quantization of the flux and the steplike structure commented in Sec. III. We shall now focus in the non-zero temperature case for few- and many-particle collective ratchets where important differences emerge.

In the few-particle case the maximum averaged center-of-mass flux is achieved for finite amplitudes and frequencies of the rocking force. Contrary to the one-particle case, the flux diminishes as the amplitude increases over its optimal value. On the other hand, we point out that for collective ratchets the maximum flux diminishes with the number of particles  $N$ . For a critical number of particles the dependence of the flux with  $N$  practically disappears, indicating the transition to the many-particle case; see Fig. 6. The value for this  $N$ -independent maximum flux that is obtained in the many-particle case coincides with the maximum flux obtained in the corresponding rocked flashing ratchet (open loop). This coincidence is analogous to the coincidence between the

maximum flux for the threshold protocol in the many-particle case and the maximum flux obtained from the corresponding flashing ratchet [10] (see also Fig. 6). Both of these coincidences can be interpreted as a consequence of the fact that these feedback protocols only use one bit of information about the system. This fact together with the increase of degrees of freedom of the system as  $N$  increases, makes that the relative strength of these feedback protocols is weakened as the number of particles  $N$  increases, and that for systems with a large number of particles those feedback protocols cannot significantly beat their open-loop counterparts. In the following we discuss the interesting cooperative effects appearing in the many-particle case.

In the many-particle case, the force per particle due to the ratchet potential,  $f(t)$  (defined in Sec. II), has a quasideterministic evolution, as fluctuations in  $f(t)$  are subdominant. The analysis of  $f(t)$  has revealed to be very helpful to understand the dynamics. For the pure feedback ratchet (without rocking) with many particles the system dynamics gets trapped with the potential “on” or “off” because the force fluctuations responsible of the switchings are negligible [4]. Consequently, the system dynamics is near equilibrium most of the time and the net force is nearly zero. This implies an average asymptotic center-of-mass velocity  $\langle \dot{x}_{CM} \rangle$  tending to zero as  $N$  increases [4]. However, the introduction of the driving force allows the system to avoid this trapping and can result in an increase of the flux.

Let us first discuss the cases of frequencies  $\Omega$  of lower or similar order to  $2\pi/T_f$ , with  $T_f$  the quasiperiod of  $f(t)$  for the pure feedback ratchet [4]. The maximum values of the flux in the many-particle case are obtained in this low-frequency regime. When the driving force is added, a complex synchronization appears between the quasideterministic dynamics of  $f(t)$  and the driving force  $A \cos(\Omega t)$ . We show in Fig. 7 [panel (a)] a typical time evolution of the forces for this case. The value of the flux depends on the details of this synchronization and it shows local maxima and minima when the system’s parameters are tuned. See panel (b) of Fig. 7, where this complex behavior is shown by computing the flux for a two-dimensional grid of  $22 \times 20$  points in the  $A$ - $\Omega$  plane. For the ratchet of Fig. 7 the maximum flux  $\langle \dot{x}_{CM} \rangle \approx 2.1$  is achieved for a driving force of amplitude  $A \approx 20$  and frequency  $\Omega \approx 55$ , expressed in units  $k_B T=1$ ,  $L=1$ ,  $\gamma=1$ . We want to call the attention to the fact that this frequency coincides with the characteristic frequency of the optimal threshold protocol [10] and of the optimal flashing ratchet  $\Omega = 2\pi/0.11 \approx 57$ . The maximum flux for the many-particle rocked feedback ratchet is reached when the rocking force has this characteristic frequency and pushes forward during the off period and backward during the on period. This makes that the ratchet potential only hinders the backward pushes of the rocking force. Contrary to the one-particle case, the flux diminishes as the amplitude increases over its optimal value; compare Fig. 4, panel (a), and Fig. 7, panel (b).

On the other hand, in the regime of large frequencies ( $\Omega \gg 2\pi/T_f$ ) the pattern of  $f(t)$  resembles the pattern for the pure feedback ratchet [4], but modulated by the high-frequency signal (Fig. 8). For moderate values of the amplitude of the rocking, the system behaves more or less as if the

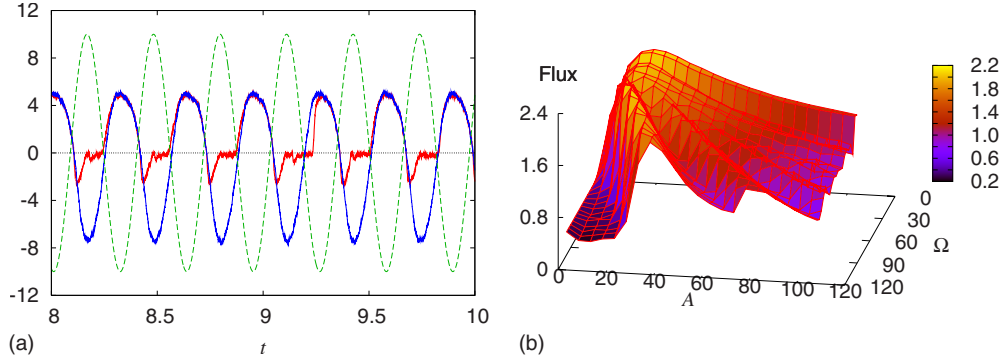


FIG. 7. (Color online) Low and medium frequency rockings in the many-particle case ( $N=10^4$ ). Panel (a): time evolution of the force  $f$  [Eq. (3)] for the rocked feedback ratchet (thick red line) and for the pure rocking ratchet (thin blue line), both with a rocking force (dashed line) of amplitude  $A=10$  and frequency  $\Omega=20$ . Panel (b): flux  $\langle \dot{x}_{CM} \rangle$  versus amplitude and frequency for the rocked feedback ratchet. We have used ratchet potential (5) with  $V_0=5$ . Units:  $k_B T=1$ ,  $L=1$ , and  $\gamma=1$ .

fluctuations were increased. Therefore, an enlargement of the flux is possible for appropriate amplitude of the driving force that succeeds in preventing the trapping similarly to the so-called threshold protocol [10]. We show in Fig. 8 this resonantlike effect for this regime. We note that for small amplitudes  $A$  the system is not able to avoid trapping, while for too large amplitudes the characteristic quasideterministic  $f(t)$  pattern is erased and the flux goes to zero.

As in the one-particle ratchet, a vibrational regime appears when the displacements induced by the driving force are faster than the effects of the other terms. This is shown in panel (b) of Fig. 8. In this panel, the dependence of the flux on the ratio  $r=A/(\gamma\Omega)$  for two different high-frequency rocking forces is compared with the flux obtained by assuming an effective dynamics defined as follows. As for the case  $N=1$ , we introduce the slow variables  $y_i(t)=x_i(t)-\psi(t)$ , with  $\psi(t)=r \sin(\Omega t)$  the displacements induced by the fast driving. Numerical simulations confirm that the dynamics in this regime is governed by the slow variables verifying the following averaged evolution equations:

$$\gamma \dot{y}_i(t) = \bar{F}_i(y_1(t), \dots, y_N(t)) + \xi_i(t), \quad (12)$$

where

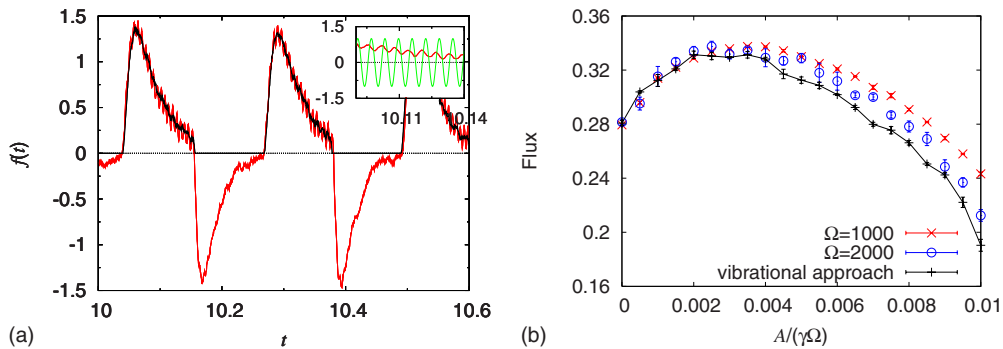


FIG. 8. (Color online) Many-particle case ( $N=10^5$ ) high-frequency rocking ( $\Omega=1000$ ) for ratchet potential (5) with  $V_0=5$ . Panel (a): evolution of the force  $f$  [Eq. (3)] for the feedback ratchet rocked with a high-frequency rocking force of amplitude  $A=1$  compared with the average force  $\sum_{i=1}^N \bar{F}_i/N$  with  $\bar{F}_i$  given by Eq. (13). We illustrate in the inset the modulation of  $f(t)$  (thick red line) due to the high-frequency rocking (thin green line). Panel (b): flux  $\langle \dot{x}_{CM} \rangle$  versus  $A/(\gamma\Omega)$  for two high-frequency rockings compared with the prediction of the vibrational approximation [Eqs. (12) and (13)]. One-sigma error bars are shown. Units:  $k_B T=1$ ,  $L=1$ , and  $\gamma=1$ .

$$\begin{aligned} \bar{F}_i(y_1, \dots, y_N) &= \frac{1}{T} \int_0^T ds \alpha(y_1 + \psi(s), \dots, y_N + \psi(s)) \\ &\quad \times F_i(y_1 + \psi(s), \dots, y_N + \psi(s)), \end{aligned} \quad (13)$$

with  $\alpha$  given by Eq. (4). This implies as before that within this regime the flux only depends on the characteristics of the driving force through the quotient  $r=A/(\gamma\Omega)$ . We have numerically checked this for the few and the many-particle cases with high-frequency driving forces, finding a better agreement in the few-particle case. However, we have also found a good agreement in the many-particle case for small values of the rocking amplitude [see Fig. 8(b)] when  $\sum_{i=1}^N \bar{F}_i/N$  is a good average description of the force  $f(t)$  [see Fig. 8(a)]. In addition to computations with ratchet potential (5), we have also performed computations with other potentials and found analogous results.

## V. CONCLUDING REMARKS

In this paper we have studied the effects of rocking a feedback ratchet. The interplay between the rocking and the feedback policy gives an intriguing rich dynamics that we have analyzed and discussed.

For the one-particle rocked feedback ratchet we have found an effective description in terms of a tilted rocking ratchet. Our simulations for rocked feedback ratchets show a relevant effect, namely, the magnification of the flux with respect to both the pure rocking and the pure feedback. That is, the rocked feedback ratchet is able to give fluxes even larger than the sum of the two fluxes separately. At this point, we remark that one of the main advantages of feedback ratchets over their open-loop counterparts is their ability to enlarge the particle flux, as it has been proved theoretically [4] and experimentally [8]. In that sense, the introduction of the fluctuating force in feedback ratchets provides a way to further enhance the flux performance. In fact, the one-particle rocked feedback ratchet studied here gives the maximum flux that has been achieved in a ratchet device without an *a priori* bias (see Fig. 6). This improvement in the flux performance is relevant for nanotechnological applications of the ratchets. In addition, the observed dependence of the flux on the frequency and amplitude of the rocking signal has been explained for the whole range of parameters of interest.

The rocking term also helps to enlarge the flux in the few- and many-particle case, as we have shown in Fig. 6. In this respect we highlight that the increase of the number of particles effectively decreases the strength of the feedback in the control, and in the limit of infinite number of particles this closed-loop protocol cannot give fluxes greater than its corresponding open-loop protocols. We have numerically shown the dependence of the flux with the amplitude and frequency of the driving force for these rocked feedback collective ratchets. The details of this dependence follow from the syn-

chronization between the driving force and the feedback. In addition, we have found a new resonantlike effect when the amplitude of the rocking is tuned in the regime of high-frequency signals. This later effect can be viewed as similar to an effective enlargement of the fluctuations in the net force, which prevents the trapping of the dynamics near equilibrium and results in an increase in the flux.

To sum up, we have proposed and discussed a closed-loop ratchet that is able to perform better than other known ratchets as a consequence of the nontrivial interplay of the feedback scheme and the rocking force. We have found an effective potential for the one-particle ratchet that explains the effective bias of the system and the *a priori* unexpected high values of the flux; it also has allowed us to provide a closed expression for the flux in the vibrational regime. We have also analyzed the rich dynamics for the collective ratchet describing the vibrational regime and new resonantlike effects.

#### ACKNOWLEDGMENTS

M.F. and F.J.C. acknowledge financial support from MCYT (Spain) through the Research Project No. FIS2006-05895, from the ESF Programme STOCHDYN, and from UCM and CM (Spain) through Grants No. CCG07-UCM/ESP-2925 and No. CCG08-UCM/ESP-4062. J.P.B. acknowledges support from the Universidad de Huelva (Project No. FQM-276) and from the Ministerio de Ciencia e Innovación (Spain) under the Research Project No. FIS2008-02873.

- 
- [1] P. Reimann, *Phys. Rep.* **361**, 57 (2002).  
 [2] J. Bechhoefer, *Rev. Mod. Phys.* **77**, 783 (2005).  
 [3] E. M. Craig, N. J. Kuwada, B. J. Lopez, and H. Linke, *Ann. Phys.* **17**, 115 (2008).  
 [4] F. J. Cao, L. Dinis, and J. M. R. Parrondo, *Phys. Rev. Lett.* **93**, 040603 (2004).  
 [5] M. Feito and F. J. Cao, *Eur. Phys. J. B* **59**, 63 (2007); F. J. Cao, M. Feito, and H. Touchette, *Physica A* **388**, 113 (2009).  
 [6] M. Bier, *Biosystems* **88**, 301 (2007).  
 [7] M. Feito and F. J. Cao, *Phys. Rev. E* **76**, 061113 (2007); E. M. Craig, B. R. Long, J. M. R. Parrondo, and H. Linke, *EPL* **81**, 10002 (2008).  
 [8] B. J. Lopez, N. J. Kuwada, E. M. Craig, B. R. Long, and H. Linke, *Phys. Rev. Lett.* **101**, 220601 (2008).  
 [9] A. L. R. Bug and B. J. Berne, *Phys. Rev. Lett.* **59**, 948 (1987); R. D. Astumian and M. Bier, *ibid.* **72**, 1766 (1994); A. Ajdari and J. Prost, *C. R. Acad., Sci, Paris II* **315**, 1635 (1992).  
 [10] M. Feito and F. J. Cao, *Phys. Rev. E* **74**, 041109 (2006).  
 [11] R. Bartussek, P. Hänggi, and J. G. Kissner, *Europhys. Lett.* **28**, 459 (1994).  
 [12] A. Ajdari, D. Mukamel, L. Peliti, and J. Prost, *J. Phys. I* **4**, 1551 (1994).  
 [13] M. O. Magnasco, *Phys. Rev. Lett.* **71**, 1477 (1993).  
 [14] S. Savel'ev, F. Marchesoni, P. Hänggi, and F. Nori, *Phys. Rev. E* **70**, 066109 (2004); M. Borromeo and F. Marchesoni, *Chaos* **15**, 026110 (2005).  
 [15] P. E. Kloeden and E. Platen, *Numerical Solution of Stochastic Differential Equations* (Springer, New York, 1992).  
 [16] I. Zapata, R. Bartussek, F. Sols, and P. Hänggi, *Phys. Rev. Lett.* **77**, 2292 (1996); F. R. Alatríste and J. L. Mateos, *Physica A* **372**, 263 (2006); W. T. Coffey, J. L. Déjardin, and Yu. P. Kalmykov, *Phys. Rev. E* **61**, 4599 (2000).  
 [17] D. Reguera, P. Reimann, P. Hänggi, and J. M. Rubí, *Europhys. Lett.* **57**, 644 (2002).  
 [18] J. L. Mateos and F. R. Alatríste, *Chaos* **18**, 043125 (2008).  
 [19] J. Plata, *Phys. Rev. E* **57**, 5154 (1998); P. Reimann, *Lect. Notes Phys.* **557**, 50 (2000).  
 [20] I. Bena, C. Van den Broeck, R. Kawai, and K. Lindenberg, *Phys. Rev. E* **66**, 045603(R) (2002); **68**, 041111 (2003).  
 [21] I. I. Blechman, *Vibrational Mechanics* (World Scientific, Singapore, 2000).  
 [22] P. S. Landa and P. V. E. McClintock, *J. Phys. A* **33**, L433 (2000); J. P. Baltanás, L. López, I. I. Blechman, P. S. Landa, A. Zaikin, J. Kurths, and M. A. F. Sanjuán, *Phys. Rev. E* **67**, 066119 (2003); J. Casado-Pascual and J. P. Baltanás, *ibid.* **69**, 046108 (2004); D. Cubero, J. P. Baltanás, and J. Casado-Pascual, *ibid.* **73**, 061102 (2006).  
 [23] M. Borromeo and F. Marchesoni *Europhys. Lett.* **72**, 362 (2005); *Phys. Rev. E* **73**, 016142 (2006).